Photocatalytic Micropatterning of Transparent Ethylsilsesquioxane−Titania Hybrid Films

Atsunori Matsuda,* Teruyuki Sasaki, Kiyoharu Tadanaga, Masahiro Tatsumisago, and Tsutomu Minami

Department of Applied Materials Science, Graduate School of Engineering, Osaka Prefecture University, Sakai, Osaka 599-8531, Japan

Received February 8, 2002. Revised Manuscript Received April 9, 2002

Refractive index of ethylsilsesquioxane−titania hybrid films increased from 1.50 to 1.55 accompanied by a decrease in film thickness by about 30% after UV light irradiation. The contact angle for water of the films decreased from 95° to about 45° and the dynamic hardness increased with UV irradiation. These changes in physical and chemical properties of the films with UV irradiation were caused by the cleavage of silicon−carbon bonds and elimination of ethyl groups in the films due to the photocatalytic effect of the titania component. Micropatterning was successfully performed on the films coated on the substrates by UV irradiation through a photomask.

1. Introduction

The micropatterning process of transparent coating films is becoming more important in the fabrication of micro-optic devices such as gratings, waveguides, and optical circuits.[1−4] The sol−gel process using metal alkoxides as starting materials has a great potential for the micropatterning of the coating films as well as for the preparation of photofunctional materials.[5−7] In the micropatterning process based on the sol−gel method, the embossing technique and photolithographic technique have been investigated so far. The former employs soft gel films, which are pressed with a stamper.[8−10] The latter uses photosensitive gel films, which are irradiated with UV light for hardening through a photomask.[11−16] In comparison with the embossing technique, the photolithographic one permits the formation of patterns with a precise shape of high resolution. Two types of photosensitive gel films, which harden because of their different photoinduced structural changes, have so far been studied. One is the gel films having carbon−carbon double bonds which undergo addition polymerization under UV light irradiation to form hard films.[11−13] The other is the gel films prepared from metal alkoxides modified with β-diketones; the chelate bonds between metal and β-diketones are cleaved with UV irradiation to produce chemically durable films.[14−16] Micropatterns can be formed in both films with carbon−carbon double bonds and with chelate bonds after UV irradiation through a photomask and subsequent etching of the films.

In the pressent study, we have found that the refractive index of sol−gel-derived ethylsilsesquioxane−titania ($EtSiO_{3/2}$−TiO_2) hybrid films increases concomitantly by a decrease in film thickness with UV light irradiation. Micropatterning based on the changes in optical thickness has been successfully carried out on the films coated on the substrates by UV irradiation through a photomask. This paper reports the changes in physical and chemical properties of the $EtSiO_{3/2}$−TiO_2 hybrid films with UV irradiation. The changes in film properties are discussed on the basis of the structural changes in the films. In addition, we describe a newly developed micropatterning process, which has great potential for designing the micro-optics components, using UV irradiation on $EtSiO_{3/2}$−TiO_2 hybrid films.

2. Experimental Section

2.1. Preparation of Hybrid Films. Preparation procedures of $80EtSiO_{3/2}$·$20TiO_2$ hybrid coating films are shown in Figure 1. Ethyltriethoxysilane ($EtSi(OEt)_3$, Shin-Etsu Chemical Industries, Tokyo, Japan) and titanium tetra-*n*-butoxide ($Ti(O\text{-}nBu)_4$, Wako Pure Chemical Industries, Osaka, Japan) were used as starting materials. $EtSi(OEt)_3$ in ethanol (EtOH) was hydrolyzed with diluted hydrochloric acid of 0.1 wt % HCl at room temperature for 30 min. The mole ratio of $EtSi(OEt)_3$: H_2O:EtOH was 0.8:4:1. $Ti(O\text{-}nBu)_4$ in EtOH was modified with

(1) Xia, Y.; Rogers, J. A.; Paul, K. E.; Whitesides, G. M. *Chem. Rev.* **1999**, *99*, 1823.
(2) Iga, K.; Misawa, *S. Appl. Opt.* **1986**, *25*, 3388.
(3) Eldada, L. *Opt. Eng.* **2001**, *40*, 1165.
(4) Schueller, O. J. A.; Whitesides, G. M.; Rogers, J. A.: Meier, M.; Dodabalapur, A. *Appl. Opt.* **1999**, *38*, 5799.
(5) Mackenzie, J. D.; Huang, Q.; Iwamoto, T. *J. Sol-Gel Sci. Technol.* **1996**, *7*, 151.
(6) Haruvy, Y.; Gilath, I. *J. Sol-Gel Sci. Technol.* **1998**, *13*, 547.
(7) Saravanamuttu, K.; Du, X. M.; Najafi, S. I.; Andrews, M. P. *Can. J. Chem.* **1998**, *76*, 1717.
(8) Tohge, N.; Matsuda, A.; Minami, T.; Matsuno, Y.; Katayama, S.; Ikeda, Y. *J. Non-Cryst. Solids* **1988**, *100*, 501.
(9) Matsuda, A.; Matsuno, Y.; Tatsumisago, M.; Minami, T. *J. Am. Ceram. Soc.* **1998**, *81*, 2849.
(10) Matsuda, A.; Sasaki, T.; Tatsumisago, M.; Minami, T. *J. Am. Ceram. Soc.* **1998**, *83*, 3211.
(11) Li, C. Y.; Chisham, J.; Andrews, M.; Najafi, S. I.; Mackenzie, J. D.; Peyghambarian, N. *Electron. Lett.* **1995**, *31*, 271.
(12) Blanc, D.; Pelissier, S.; Saravanamuttu, K.; Najafi, S. I.; Andrews, M. P. *Adv. Mater.* **1999**, *11*, 1508.
(13) Tadanaga, K.; Ellis, B.; Sedddon, A. B.; *J. Sol-Gel Sci. Technol.* **2000**, *19*, 687.
(14) Tohge, N.; Shinmou, K.; Minami, T. *J. Sol-Gel Sci. Technol.* **1994**, *2*, 581.
(15) Kintaka, K.; Nishii, J.; Tohge, N. *SPIE Proc. Sol−Gel Optics V* **2000**, *38*, 3943.
(16) Yamada, N.; Yoshinaga, I.; Katayama, S. *J. Appl. Phys.* **1999**, *85*, 2423.

10.1021/cm020118+ CCC: $22.00
Published on Web 05/10/2002

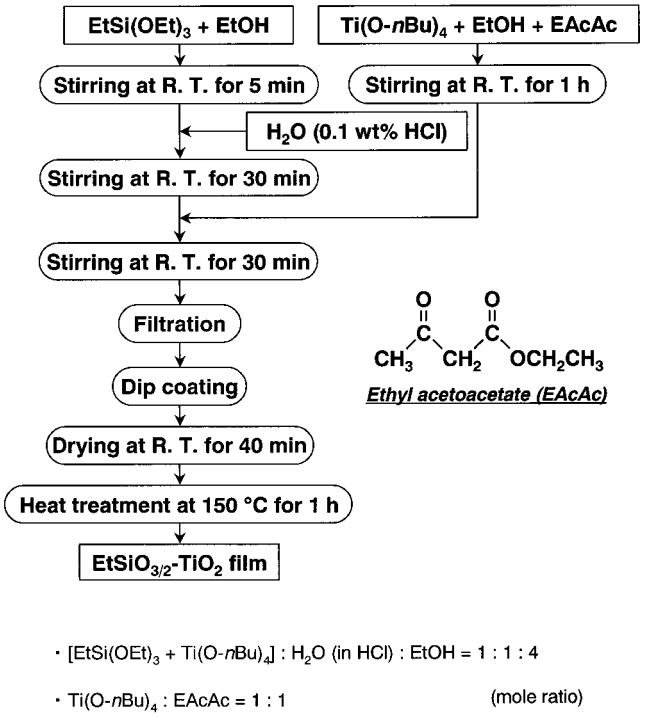

Figure 1. Preparation procedures of $80EtSiO_{3/2}{\cdot}20TiO_2$ hybrid coating films.

ethyl acetoacetate (EAcAc, Kishida Chemical, Osaka, Japan) by stirring the solution at room temperature for 1 h. The mole ratio of Ti(O-*n*Bu)$_4$:EtOH:EAcAc was 1:20:1. The modified Ti(O-*n*Bu)$_4$ solution was added to the hydrolyzed Si(OEt)$_4$ solution and stirred continuously for 30 min. The clear sols obtained were filtered using a 0.45-μm filter (GL Chromato Disk, Kurabo, Osaka, Japan) and served as coating solutions.

Composite films derived from a mixture of $EtSiO_{3/2}$ sol at 80 mol % and commercially available anatase TiO_2 sol at 20 mol % were also prepared for comparison. The $EtSiO_{3/2}$ sol was prepared in a manner simlar to that described in Figure 1. Commercially available TiO_2 sol adopted was Partitan 5610 (Nihon Parkerizing, Tokyo, Japan), which is an aqueous sol containing 10 wt % anatase nanocrystals of about 10 nm in diameter.

The coating was carried out by dipping−withdrawing of a substrate with a speed of 0.45 or 1.11 mm/s in an ambient atmosphere. Silica glass plates, soda−lime−silica glass plates, and silicon wafers were used as the substrates for coating. The substrates coated with films were dried at room temperature for 40 min and then heat-treated mainly at 150 °C for 1 h.

UV light irradiation against the coating films was carried out using an ultra-high-pressure mercury lamp (UIS-25102 250W, Ushio, Tokyo, Japan) with an optical fiber bundle and a condensing lens. Irradiation intensity for the coating films was measured using an illumination photometer (UIT-150-A, Ushio, Tokyo, Japan) with detectors S365 and S254. The intensities of the UV light irradiated were 82 mW/cm^2 in a range of 310−390 nm and 22 mW/cm^2 in a range of 220−310 nm. The maximum temperature of the films coated on glass substrates during UV light irradiation for 240 min under the conditions above was lower than 50 °C, which was monitored using a thermocouple.

2.2. Characterization of Hybrid Films. Ultraviolet−visible (UV−vis) transmission spectra of the film, which was coated on one side of silica glass or soda−lime−silica glass were obtained using a UV−vis spectrophotometer (V-560, JASCO, Tokyo, Japan). The refractive index and thickness of the film were calculated from wavy patterns due to the interference between the film and the substrate.[17] In the calculation, refractive indices of 1.46 and 1.52 were adopted for silica glass and soda−lime−silica glass, respectively. Changes in microhardness and contact angle for water of the coating films with UV light irradiation were measured using a dynamic ultra microhardness tester (DUH-W201, Shimadzu, Kyoto, Japan) and a contact angle meter (CA-C, Kyowa surface science, Tokyo, Japan), respectively.

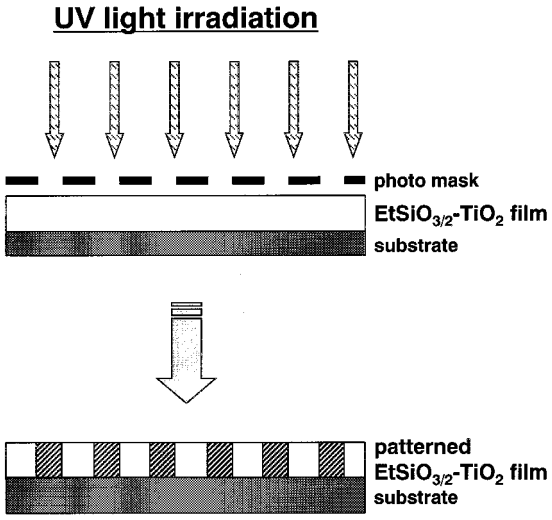

Figure 2. Schematic illustration of the micropatterning process on coating films with UV light irradiation.

Fourier transformed infrared (FT-IR) absorption spectra of the films coated on silicon substrates were measured in transmission mode using an FT-IR spectrophotometer (FT-IR1650, Perkin-Elmer, CT). X-ray diffraction (XRD) patterns of the coating films before and after UV irradiation were measured using an X-ray diffractometer (M18XHF22−SRA, Mac science, Tokyo, Japan). Structural units of the coating films before and after UV light irradiation were examined using a ^{29}Si cross-polarization magic-angle spinning (CPMAS)-NMR (Varian Model Unity Inova 300) technique. The sample powders were obtained by scratching the films off the substrates. The NMR spectra were measured at 59.59 MHz, 4.7 μs of 90° pulse length, 10 s of decay between pulses, and a spinning rate of 3000−4000 Hz. Tetramethylsilane was used as an external standard. The texture of the coating films before and after UV light irradiation was observed using a field-emission-type scanning electron microscope (FE-SEM) (S-4500, Hitachi, Tokyo, Japan) and a field-emission-type transmission electron microscope (FE-TEM) (HF-2000, Hitachi, Tokyo, Japan).

2.3. Micropatterning on Hybrid Films with UV Light Irradiation. A schematic illustration of the micropatterning process on coating films with UV light irradiation is shown in Figure 2. UV light was irradiated to the film coated on the substrate through a photomask. Metal meshes with 30-μm squares through holes in 60-μm pitch were mainly used as a photomask.

The surface of the patterned film with UV irradiation was observed on an optical microscope (Model BX50, Olympus, Tokyo, Japan). The three-dimensional shapes of the micropatterns formed in the films were evaluated using atomic force microscopy (AFM) (Nanopics, Seiko instrument, Tokyo, Japan) and a three-dimensional surface profilometer (TDA-22, Kosaka laboratory, Tokyo, Japan).

3. Results and Discussion

3.1. Changes in Physical and Chemical Properties of Hybrid Films. Titania-containing inorganic−organic materials have been extensively studied for their application to optical coatings and micro-optic devices because of their high refractive indices as well as good thermal and chemical durability.[18−21] However,

(17) Yoldas, B. E. *Appl. Opt.* **1980**, *19*, 1425.
(18) Sorek, Y.; Reisfeld, R. *Appl. Phys. Lett.* **1993**, *63*, 3256.
(19) Que, W.; Sun, Z.; Zhou, Y.; Lam, Y. L.; Chan, Y. C.; Kam, C. H. *Thin Solid Films* **2000**, *358*, 16.
(20) Yamada, N.; Yoshinaga, I.; Katayama, S. *J. Sol-Gel Sci. Technol.* **2000**, *17*, 123.

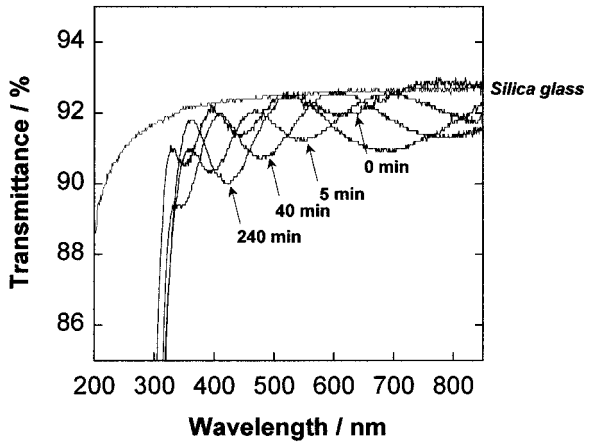

Figure 3. Optical transmission spectra of the $80EtSiO_{3/2}$·$20TiO_2$ hybrid films coated on one side of the silica glass substrates which were heat-treated at 150 °C for 1 h and irradiated with UV light for various periods of time.

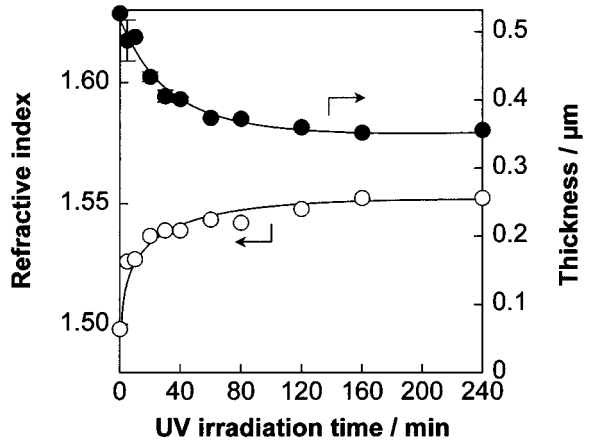

Figure 4. Refractive index and thickness of the films irradiated with UV light for various periods of time.

little is known about the changes in optical properties of the titania-containing inorganic−organic hybrid films with UV irradiation.

Figure 3 shows optical transmission spectra of the $80EtSiO_{3/2}$·$20TiO_2$ hybrid films coated on one side of the silica glass substrates which were heat-treated at 150 °C for 1 h and irradiated with UV light for various periods of time. The maxima of wavy patterns of the transmission spectra are as high as the transmittance of the substrate without a coating film, so that the films are highly transparent even after the UV irradiation. The minima of transmission wavy patterns decrease and shift to shorter wavelengths with UV irradiation, indicating that the refractive index of the films increases and the film thickness decreases with UV irradiation. The refractive index and thickness of the films irradiated with UV light for various periods of time are calculated from these optical transmission spectra and shown in Figure 4. After UV light irradiation for 240 min, the refractive index increases from 1.50 to 1.55 accompanied by a relatively large decrease in film thickness by about 30% from 0.79 to 0.55 μm. These phenomena indicate that the films were densified with UV irradiation.

(21) Que, W.; Zhou, Y.; Lam, Y. L.; Chan, Y. C.; Cheng S. D.; Sun, Z.; Kam, C. H. *J. Sol-Gel Sci. Technol.* **2000**, *18*, 77.

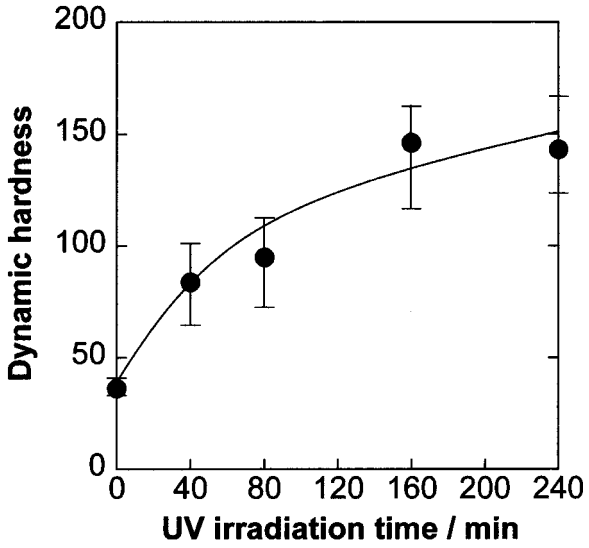

Figure 5. Changes in dynamic hardness of the $80EtSiO_{3/2}$·$20TiO_2$ hybrid films with UV light irradiation time.

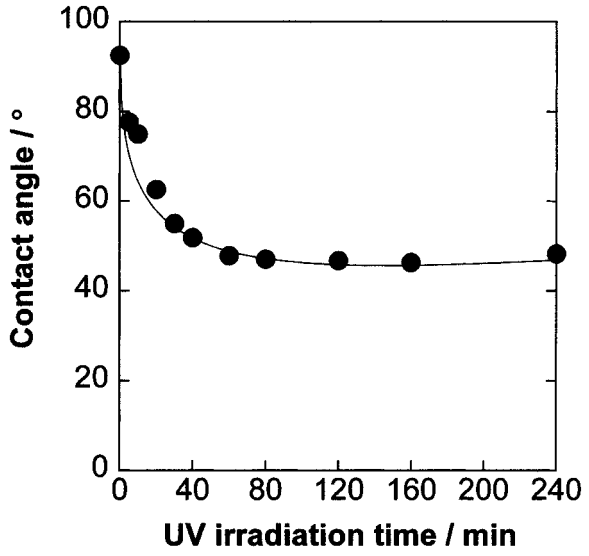

Figure 6. Changes in contact angle for water of the $80EtSiO_{3/2}$·$20TiO_2$ hybrid film with UV light irradiation time.

Figure 5 shows changes in dynamic hardness of the $80EtSiO_{3/2}$·$20TiO_2$ hybrid films with UV irradiation time. The hardness of the film increases with UV irradiation time. The increase in hardness of the films must reflect the densification of the films. The hardness of polystyrene substrates was ca. 20 under the same conditions. The $EtSiO_{3/2}$−TiO_2 hybrid films can be formed not only on glass and metals but also on plastics so that the films are promising as protective coatings and hard coatings for plastic substrates and goggles.

Figure 6 shows changes in the contact angle for water of the $80EtSiO_{3/2}$·$20TiO_2$ hybrid film with UV light irradiation time. The contact angle for water of the film steeply decreases from 95° to about 50° in 40 min and gradually to 45° in 240 min. The decrease in contact angle for water indicates that the amount of organic groups at the surface of the film decreased with UV irradiation. The tendency of the decrease in the contact angle for water of the film with UV irradiation corresponds to those of the changes in optical properties (Figure 4) and in dynamic hardness (Figure 5) of the films. This suggests that the contact angle for water was

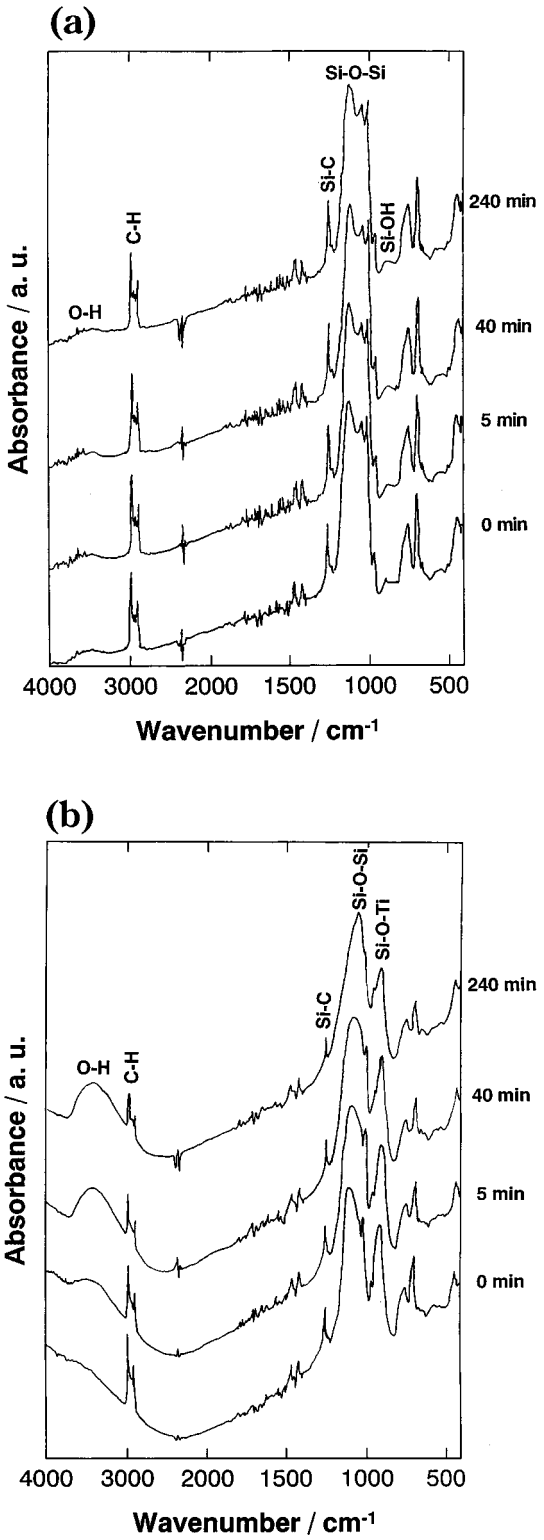

Figure 7. FT-IR absorption spectra of (a) $EtSiO_{3/2}$ films and (b) $80EtSiO_{3/2}{\cdot}20TiO_2$ hybrid films coated on silicon substrates and irradiated with UV light for 0, 5, 40, and 240 min.

lowered not only at the surface but also inside of the films. Almost no changes have been observed in optical properties, dynamic hardness, and contact angle of water for the pure $EtSiO_{3/2}$ films during UV irradiation under the same conditions. Therefore, the changes in physical and chemical properties of $80EtSiO_{3/2}{\cdot}20TiO_2$ hybrid films with UV irradiation are obviously achieved by the incorporation of the TiO_2 component into $EtSiO_{3/2}$.

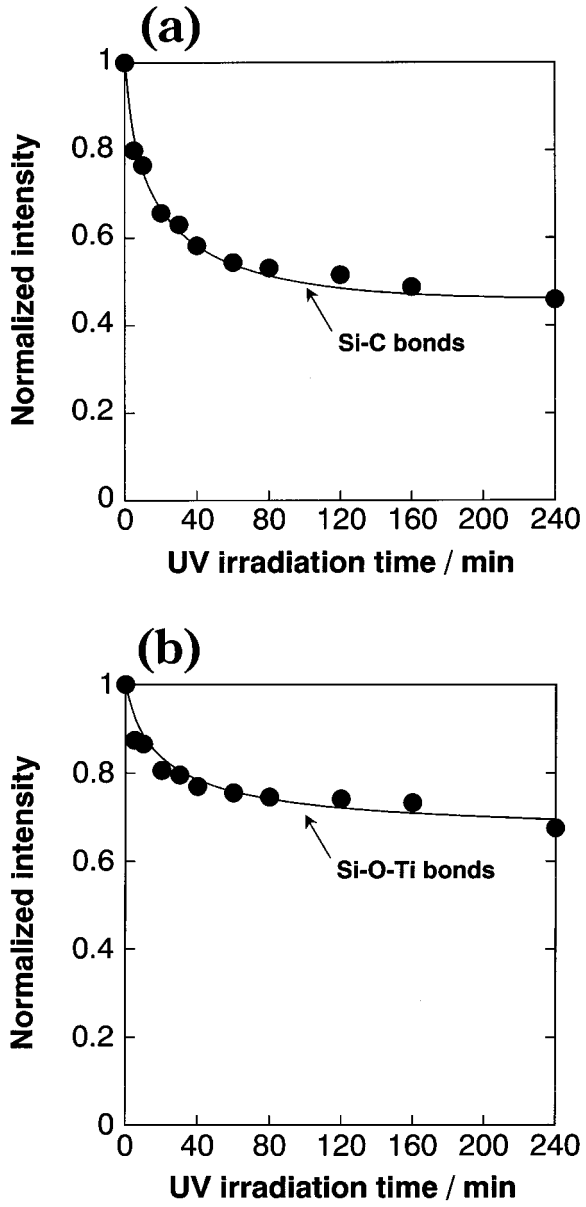

Figure 8. Changes in the normalized intensities of the absorption peaks (a) at 1253 cm^{-1} due to Si−C bonds and (b) at 904 cm^{-1} due to Si−O−Ti bonds in the FT-IR spectra of $80EtSiO_{3/2}{\cdot}20TiO_2$ hybrid films with UV light irradiation. The intensities of the absorption peaks were normalized with those of the films before UV light irradiation.

3.2. Structural Changes of Hybrid Films with UV Light Irradiation. The refractive index of $EtSiO_{3/2}$−TiO_2 hybrid films increased concomitantly by a decrease in film thickness after UV light irradiation (Figure 4). The contact angle for water of the films decreased (Figure 5) and the dynamic hardness increased (Figure 6) with UV irradiation. In this section, these changes in physical and chemical properties of the $EtSiO_{3/2}$−TiO_2 hybrid films with UV irradiation are discussed on the basis of the structural changes in the films.

The thermal decomposition of Ti−EAcAc complex and disappearance of EAcAc in the films at 80 °C were confirmed from IR absorption spectra. Therefore, EAcAc used for chemical modification of Ti(O-*n*Bu)$_4$ has little influence on the changes in optical properties, contact angle for water, and dynamic hardness of the $EtSiO_{3/2}$−

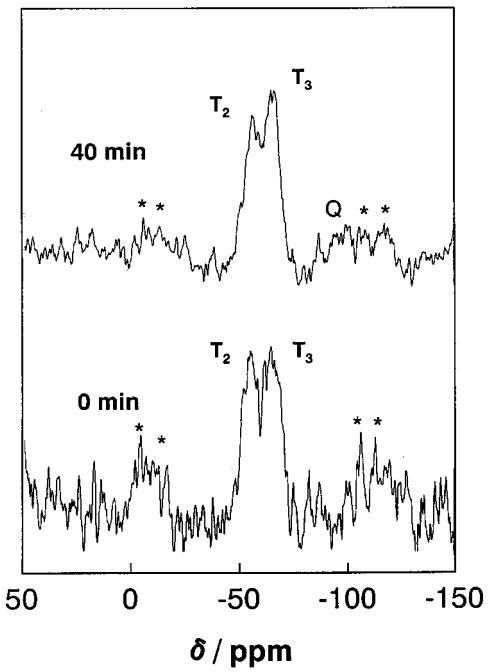

Figure 9. ^{29} Si CPMAS NMR spectra of $80EtSiO_{3/2}$·$20TiO_2$ hybrid powders before and after the UV light irradiation 40 min. *: spinning sidebands.

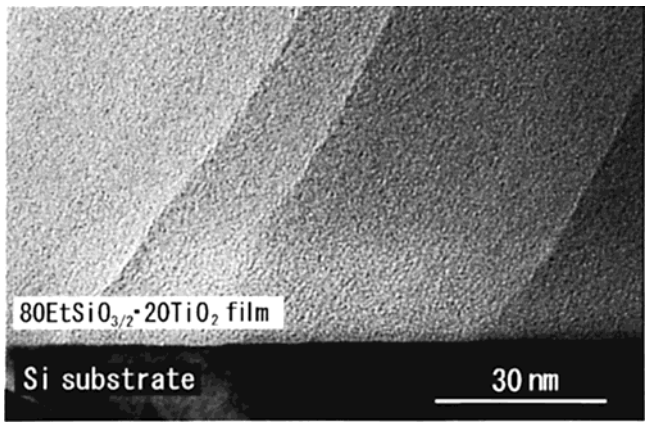

Figure 10. TEM image of a $80EtSiO_{3/2}$·$20TiO_2$ hybrid film coated on a Si substrate and irradiated with UV light for 240 min.

TiO_2 films, which were heat-treated at 150 °C, with UV irradiation.

Figure 7 shows FT-IR absorption spectra of (a) $EtSiO_{3/2}$ films and (b) $80EtSiO_{3/2}$·$20TiO_2$ hybrid films coated on silicon substrates and irradiated with UV light for 0, 5, 40, and 240 min. Both films were heat-treated at 150 °C for 1 h before UV irradiation. In the FT-IR spectra of $EtSiO_{3/2}$ films (Figure 7a), a broad absorption band at around 1100 cm^{-1} and a weak band at 880 cm^{-1} can be assigned to Si−O−Si bonds and Si−OH bonds, respectively. Sharp peaks at 1253 and 2900 cm^{-1} are respectively assigned to Si−C bonds and C−H bonds of ethyl groups in the films. Almost no changes are observed for the FT-IR spectra in Figure 7a with UV irradiation. On the other hand, the intensities of absorption peaks at 1253 cm^{-1} due to Si−C bonds and at 2900 cm^{-1} due to C−H bonds in the spectra of $80EtSiO_{3/2}$·$20TiO_2$ hybrid films decrease with UV light irradiation accompanied by a decrease in the intensity of an absorption peak at 904 cm^{-1} due to Si−O−Ti bonds in which titanium ions are incorporated in the four-coordinated state[22,23] (Figure 7b). In addition, the intensity of a band at around 3400 cm^{-1} due to OH bonds increases concomitantly by these spectral changes during UV light irradiation. These results indicate that ethyl groups in the $80EtSiO_{3/2}$·$20TiO_2$ hybrid film were eliminated after the cleavage of Si−C bonds and the dissociation of Si−O−Ti bonds followed by the formation of Si−OH groups and/or Si−O−Si bonds. It is obvious from the comparison with Figure 7a,b that the cleavage of Si−C bonds with UV irradiation is achieved by the incorporation of the TiO_2 component into $EtSiO_{3/2}$. This new finding suggests that these structural changes of the films with the UV irradiation occur because of the photocatalytic activity of the TiO_2 component.

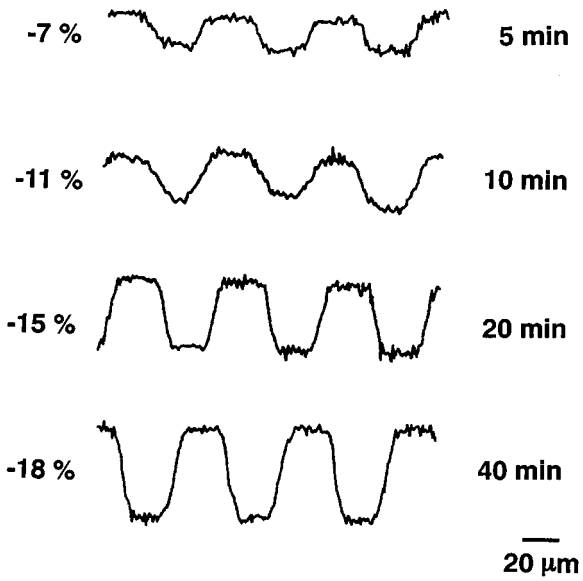

Figure 11. Surface profiles of the $80EtSiO_{3/2}$·$20TiO_2$ hybrid film irradiated with UV light for 5, 10, 20, and 40 min through the photomask. The profiles were obtained using a surface profilometer.

Figure 8 shows the changes in the normalized intensities of the absorption peaks (a) at 1253 cm^{-1} due to Si−C bonds and (b) at 904 cm^{-1} due to Si−O−Ti bonds in the FT-IR spectra of $80EtSiO_{3/2}$·$20TiO_2$ hybrid films with UV light irradiation. The intensities of the absorption peaks were normalized with those of the film before UV irradiation. The intensity of the peak at 1253 cm^{-1} due to Si−C bonds decreases with UV irradiation in 240 min to become 0.45 of that of the film before the irradiation (Figure 8a). The decrease in the intensity of the peak due to Si−C bonds with UV irradiation is accompanied by the decrease in the intensity of a peak at 2900 cm^{-1} due to C−H bonds as shown in Figure 7b. Therefore, the cleaved ethyl groups probably leave the film immediately after UV irradiation. The intensity of the peak at 904 cm^{-1} due to Si−O−Ti bonds decreases with UV irradiation in 240 min to become about 0.7 of that of the film before the irradiation (Figure 8b). The decrease in the intensity of the peak at 904 cm^{-1} suggests that Si−O−Ti bonds are dissociated with UV irradiation. The tendency of the decrease in the amounts of Si−C bonds shown in Figure 8a is analogous to that

(22) Mukherjee, S. P. *J. Non-Cryst. Solids* **1980**, *42*, 477.
(23) Morikawa, H.; Osuka, T.; Marumo, F.; Yasumori, A.; Yamane, M. *J. Non-Cryst. Solids* **1986**, *82*, 97.

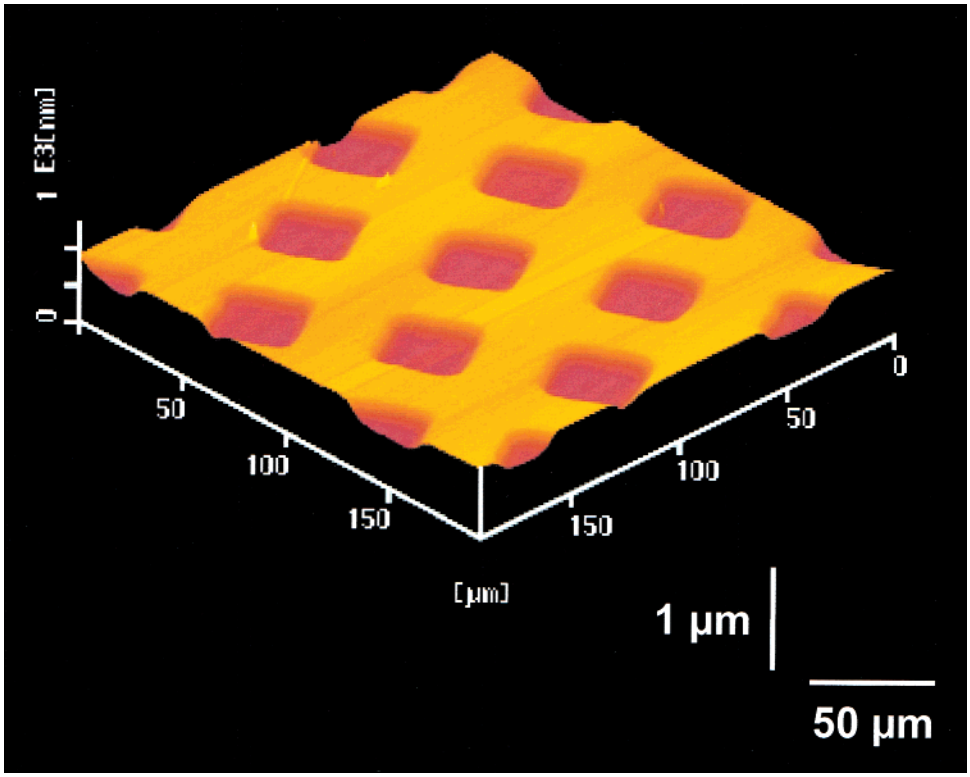

Figure 12. AFM image of the surface of the $80EtSiO_{3/2}$·$20TiO_2$ hybrid film after UV light irradiation through the photomask for 40 min.

in the amounts of Si−O−Ti bonds shown in Figure 8b, indicating that dissociation of Si−O−Ti bonds is closely related to the photocatalytic cleavage of Si−C bonds.

XRD measurement showed that both $80EtSiO_{3/2}$·$20TiO_2$ hybrid films before and after UV irradiation were amorphous. It is noteworthy that cleavage of Si−C bonds with UV light irradiation occurred owing not to titania crystals but to amorphous titania component in which titanium ions were incorporated in a four-coordinated state in silsesquioxane as shown by IR absorption spectra (Figure 7b).

Imai et al. have reported that TiO_2 gel films are densified by irradiation of photons with energies higher than the band gap of about 4 eV, which corresponds to UV light of 310 nm.[24,25] The densfication of the TiO_2 films is considered to be induced by the bond cleavage via the electronic excitation from the valence band to conduction band. In the present $EtSiO_{3/2}$−TiO_2 hybrid films, the absorption edge of the film was found from preliminary experiments to shift to a lower energy level, that is, longer wavelength, with an increase in the TiO_2 content. In addition, the cleavage of Si−C bonds in pure $EtSiO_{3/2}$ was hardly observed in the IR absorption spectra even after UV irradiation under the same conditions. Therefore, the TiO_2 component incorporated with the films absorbs UV light and the excited electrons probably cleave the Si−C bonds. From IR absorption spectra, Si−O−Ti bonds in SiO_2−TiO_2 films derived from tetraethoxysilane and Ti(O-*n*Bu)$_4$ did not dissociate with UV irradiation. This suggests that the cleavage of Si−C bonds should induce the dissociation of Si−O−Ti bonds in the $EtSiO_{3/2}$−TiO_2 hybrid films, resulting in the densification of the films.

We have carried out two kinds of experiments to clarify the feature of the photocatalytic cleavage of the Si−C bond in the hybrid $EtSiO_{3/2}$−TiO_2 films. One is the investigation of the structural changes of the composite films derived from a mixture of $EtSiO_{3/2}$ sol at 80 mol % and commercially available anatase TiO_2 sol at 20 mol %. The intensity of the peak at 1290 cm^{-1} due to Si−C bonds in the composite film decreased with UV light irradiation and became 0.6 of that of the film in 240 min. The degree of the cleavage of Si−C bonds in the composite film is smaller than that of the alkoxide-derived $EtSiO_{3/2}$−TiO_2 hybrid film as shown in Figure 8b. It was found that the intensity of the IR absorption peak at around 900 cm^{-1} due to Si−O−Ti bonds in the composite film was much smaller than that of the hybrid film. This result suggests that excited electrons from the TiO_2 component in the hybrid film derived from alkoxides photocatalytically cleave the Si−C bonds more effectively than those in the composite film derived from the mixture of $EtSiO_{3/2}$ sol and anatase sol.

As the other experiment, the structural changes of the $EtSiO_{3/2}$ film on a Ti(O-*n*Bu)$_4$-derived TiO_2 anatase lower layer during UV irradiation have also been examined. The values of thickness of the $EtSiO_{3/2}$ upper layer and the TiO_2 anatase lower layer were 570 and 50 nm, respectively. The photocatalytic decomposition of surface organic groups on a TiO_2 lower layer has been reported so far.[26−28] However, the cleavage of Si−C

(24) Imai, H.; Awazu, K.; Yasumori, M.; Onuki, H.; Hirashima, H. *J. Sol-Gel Sci. Technol.* **2000**, *8*, 365.
(25) Imai, H.; Hirashima, H.; Awazu, K. *Thin Solid Films* **2000**, *351*, 91.
(26) Tada, H. *Langmuir* **1996**, *12*, 966.
(27) Tada, H.; Tanaka, M. *Langmuir* **1997**, *13*, 360.
(28) Tadanaga, K.; Morinaga, J.; Matsuda, A.; Minami, T. *Chem. Mater.* **2000**, *12*, 590.

bonds and the formation of OH bonds were not observed after UV irradiation in this study, so the $EtSiO_{3/2}$ upper layer is too thick to be transformed into silica films by the photocatalytic effect of the TiO_2 lower layer.

From the two experiments above, the feature of $EtSiO_{3/2}$−TiO_2 hybrid films is clarified as follows: (1) photocatalytic cleavage of Si−C bonds in alkoxide-derived $EtSiO_{3/2}$−TiO_2 hybrid films with UV light irradiation occurs more readily than that in the $EtSiO_{3/2}$−TiO_2 composite films derived from a mixture of $EtSiO_{3/2}$ sol and anatase TiO_2 sol, and (2) the hybridization of $EtSiO_{3/2}$ and TiO_2 components permits the photocatalytic cleavage of Si−C bond in the whole of the films.

Figure 9 shows ^{29}Si CPMAS NMR spectra of $80EtSiO_{3/2}$·$20TiO_2$ hybrid powders before and after the UV light irradiation for 40 min. In the spectra of the powders before UV irradiation, two bands are observed at −55 and −65 ppm, which are assigned to the silicon atom with two bridging oxygens (T_2 unit) and the silicon atom with three bridging oxygens (T_3 unit), respectively. The intensity of the band due to T_3 units is almost the same as that of the band due to T_2 units before UV irradiation. After UV irradiation for 40 min, the intensity of the band due to T_3 units becomes larger than that of the band due to T_2 units, indicating that Si−O−Si bonds were formed to develop the network structure in the film with UV irradiation. It is not so clear because of the overlapping of spinning sidebands but a very broad band is newly observed at around −100 ppm after UV irradiation. This band is probably assigned to the silicon atom with three or four bridging oxygens (Q^3 or Q^4 unit). These results suggest that the Si−C bond in the films cleaved with UV irradiation and changed into Si−OH or Si−O−Si bond.

Figure 10 shows a TEM image of $80EtSiO_{3/2}$·$20TiO_2$ hybrid film coated on a Si substrate which was irradiated with UV light for 240 min. No crystalline phases and no inhomogenieties are observed in the films even after UV light irradiation for 240 min. The TEM observation results agreed with the XRD halo patterns for the films. Therefore, the resultant films were amorphous without titania nanocrystallites. The cleavage of Si−C bonds with UV irradiation occurred owing not to titania nanocrystals but to the amorphous titania component in which titanium ions were incorporated in a four-coordinated state in ethylsilsesquioxane.

3.3. Photocatalytic Micropatterning of Hybrid Films. UV light was irradiated on the $80EtSiO_{3/2}$·$20TiO_2$ hybrid film coated on the substrate using a metal mesh with 30-μm squares through holes in 60-μm pitch as a photomask. Figure 11 shows the surface profiles of the films irradiated with UV light through the photomask for 5, 10, 20, and 40 min. When UV light has been irradiated on the film for 5 min, the surface profile is still dull. The surface profile becomes distinct with UV light irradiation and a sharp profile with a shrinkage of about 20% is obtained in 20 min. After UV light irradiation for 40 min, the surface profile remains almost unchanged. This micropatterning process is based on the irreversible structural changes in the hybrid films caused by the cleavage of Si−C bonds during UV irradiation. Therefore, the shape of the resultant patterns is quite stable upon storage for a long period of time.

The AFM image of the surface of the film after UV light irradiation for 40 min is shown in Figure 12. Arrayed dark squares are concave areas, which correspond to the through holes of the metal mesh used as a photomask. The depth of the concave areas was 0.11 μm, which was 18% of the initial thickness (0.62 μm) of the film before UV irradiation. The shrinkage of 18% in the areas on which UV light was irradiated through the photomask is smaller than that (33%) of the film after UV light irradiation without a photomask. Thus, the shrinkage of the UV light irradiated area probably becomes smaller when the resolution of the photomask patterns is higher. The relationship among refractive index change, shrinkage, and mask resolution is now under study.

As shown in Figure 4, UV light irradiated areas show a higher refractive index than that of the UV light unirradiated area. Therefore, micropatterns and microdots based on the refractive index change can be formed in the films using this process. In other words, this process has great potential as a micropatterning process to fabricate flat-type and integrated-type micro-optic and photonic components such as gratings, waveguides, and optical circuits. Moreover, UV light irradiated areas show higher hardness and smaller contact angle for water, that is, higher wettability, than those of the UV light unirradiated area as shown in Figures 5 and 6. In the preceding paper,[28] we have reported the fabrication of superhydrophobic−superhydrophillic micropatterns based on fluoroalkylsilane/titania/flowerlike alumina multilayers on substrates and UV irradiation on the selected area for them through a photomask. Only the UV light irradiated areas become hydrophillic because of the elimination of fluoroalkyl groups by the photocatalytic effect of the titania lower layer, while the unirradiated areas remain hydrophobic. One of the promising applications of such hydrophobic−hydrophilic micropatterns is the microprinting process in which the printing plate holds ink on the hydrophilic areas and the plate imprints it on another surface. The hydrophobic−hydrophilic patterns of the $EtSiO_{3/2}$−TiO_2 hybrid films in the present work are also applicable to microprinting. The thickness of $EtSiO_{3/2}$−TiO_2 hybrid films can be increased up to about 1 μm, so the abrasion resistance in repeated printings is expected for the patterned films, which were fabricated on a printing plate.

Conclusions

We have found that the refractive index of the $80EtSiO_{3/2}$·$20TiO_2$ hybrid film increased from 1.50 to 1.55 accompanied by a decrease in film thickness by about 30% after UV light irradiation. The contact angle for water of the film decreased from 95° to about 45° and the dynamic hardness of the film increased with UV light irradiation. Ethyl groups in the $80EtSiO_{3/2}$·$20TiO_2$ film were eliminated after the cleavage of Si−C bonds and the dissociation of Si−O−Ti bonds to form Si−OH groups and/or Si−O−Si bonds with UV irradiation. These structural changes of the films with UV irradiation occur by the photocatalytic activity of the TiO_2 component. The TiO_2 component incorporated with the films absorbs UV light and the excited electrons probably cleave the Si−C bonds. The cleavage of Si−C

bonds should induce the dissociation of Si−O−Ti bonds, resulting in the densification of the films. No crystalline phases and no inhomogenieties are observed in the films ever after UV irradiation. The cleavage of Si−C bonds with UV irradiation occurred owing not to titania nanocrystals but to the amorphous titania component in which titanium ions were incorporated in a four-coordinated state in silsesquioxane. Micropatterning was successfully carried out on the $80EtSiO_{3/2}{\cdot}20TiO_2$ hybrid film coated on the substrate by UV light irradiation through a photomask. This micropatterning process has great potential for fabrication of the micro-optic and photonic components as well as for application to microprinting.

Acknowledgment. This work was supported by a Grant-in-Aid from the Ministry of Education, Culture, Sports, Science and Technology of Japan.

CM020118+